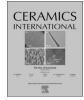
Contents lists available at ScienceDirect





Ceramics International

journal homepage: www.elsevier.com/locate/ceramint

Theoretical and experimental analyses of thermal properties of porous polycrystalline mullite



Yoshihiro Hirata*, Yusuke Kinoshita, Taro Shimonosono, Tomohiro Chaen

Department of Chemistry, Biotechnology, and Chemical Engineering, Kagoshima University, 1-21-40 Korimoto, Kagoshima 890-0065, Japan

ARTICLE INFO

Keywords: A. Hot pressing B. Porosity C. Thermal conductivity D. Mullite

ABSTRACT

This paper examined experimentally and theoretically the thermal diffusibility (α), heat capacity (C_{P1}) at a constant pressure (1 atm, 101.33 kPa) and thermal conductivity (κ = $C_{P1}\alpha$) for the porous mullite ceramics with 0–55% porosity in a wide temperature range from 298 to 1073 K. The change in the κ values with temperature or porosity for the porous mullite was similar to the temperature dependence or porosity dependence of the α values, which were greatly reduced by the air included in the pores. The κ values for the porous mullite were theoretically analyzed with two model structures of pore–dispersed mullite continuous phase system (A model) and mullite–dispersed pore continuous phase system (B model). The measured κ values at 0–23% porosity agreed well with the κ values deviated for model A structure. In the high porosity range from 33% to 55%, the measured κ values deviated from the κ curve calculated for model A structure of 30–60% porosity is equivalent to the mixed microstructure of model A and model B for the thermal conductivity measuremt.

1. Introduction

Porous ceramics with a high melting point, a high porosity and high chemical stability is useful as a refractory material for the steel industry, catalyst supports or gas filters used at high temperatures. The physicochemical properties of a porous ceramic material are basically dominated by the characteristics of the connected solid part and the gases included in the tortuous pores. That is, the property of a porous ceramic material may be expressed as functions of the characteristics of the solid part and gases and the pore structure. In our previous papers [1-7], theoretical mixing rules of the thermal conductivity (κ), Young's modulus (E) and thermal expansion coefficient (β) have been derived for the multiphase material. These mixing rules are also applicable to the porous material when the gas phase in the pores is treated as a constituent phase (κ (gas) \neq 0 W/mK, E(gas)=0 GPa, β (gas)=0 m/mK). For instance, the thermal conductivity (κ_{ap} , Eq. (1)) of two phase system can be expressed by three parameters of κ_1 for inclusion, κ_2 for a continuous phase and volume fraction of V_1 of inclusion [1].

$$\kappa_{ap} = \kappa_2 - \kappa_2 V_1^{2/3} \left[1 - \frac{1}{1 - V_1^{1/3} \left\{ 1 - \frac{\kappa_2}{\kappa_1} \right\}} \right]$$
(1)

п

This equation results in the following value: $\kappa_{ap}{=}\kappa_2$ for V1=0, $\kappa_{ap}{=}\kappa_1$ for V1=1.

In the three phase system (continuous phase 2 with volume fraction V₂, dispersed phase 1 with volume fraction V₁, and dispersed phase 3 with volume fraction V_3), the thermal conductivity (κ_{ap}) of the continuous phase including a dispersed phase 1 is calculated by Eq. (1). The V_1 value in Eq. (1) is changed to the ratio of $V_1/(V_1+V_2)$ for the two phase system of phases 1 and 2. The calculated κ_{ap} is again substituted for κ_2 in Eq. (1) and the values κ_1 and V_1 are changed to κ_3 and V₃, respectively, for the microstructure where a phase 3 is dispersed in the continuous phase including a dispersed phase 1. Therefore, the repeat of Eq. (1) two times provides the effective thermal conductivity (κ_b) of three phase composite. In our previous papers [1– 4], it was clarified that the derived κ_{ap} or κ_b equation explains well the thermal conductivities measured at room temperature for the AlN particles-dispersed SiO₂ continuous phase system [1] and the refractory brick of carbon-alumina-pore system [2], carbon-aluminasilicon carbide-pore system [2], carbon-alumina-silica-pore system [2], alumina-mullite-pore system [3] and silicon carbide-oxide additive-pore system [4].

Based on the above results, this paper focuses on the validation of Eq. (1) for porous mullite ceramics in a wide porosity range from 0% to 55% and in a heating temperature range from 298 to 1073 K. Mullite $(3Al_2O_3 \cdot 2SiO_2)$ is the only stable compound with high covalency in the

* Corresponding author.

E-mail address: hirata@cen.kagoshima-u.ac.jp (Y. Hirata).

http://dx.doi.org/10.1016/j.ceramint.2017.05.009

Received 6 April 2017; Received in revised form 2 May 2017; Accepted 2 May 2017 Available online 03 May 2017

0272-8842/ \odot 2017 Elsevier Ltd and Techna Group S.r.l. All rights reserved.

SiO₂–Al₂O₃ system [8–10]. Its thermal or physicochemical properties [11–14], such as high melting point (2101 ± 10 K), low thermal expansion coefficient ($3.5 \times 10^{-6} - 5.9 \times 10^{-6}$ m/mK at 298–1273 K) [6], good thermal shock fracture resistance, low true density (3.16–3.22 g/ cm³ for 70.5–74.0 mass% Al₂O₃ mullite solid solution) [11], high creep resistance and good chemical stability, can be compared with the properties of Si₃N₄ or SiC in terms of high temperature structural materials application. The thermal conductivities measured in the present porous mullite were well interpreted with the κ_{ap} values by Eq. (1) for two model structures of pore-dispersed mullite continuous phase system and mullite-dispersed pore continuous phase system. That is, the thermal conductivity for the mullite–open pore system is well represented using the κ values calculated for the above two model structures.

2. Experimental procedure

The following two kinds of mullite powders were mixed to control the porosity and pore size distribution of a sintered mullite compact: powder 1 (Chemical Vapor Deposition process mullite)-median particle size of 80 nm, chemical composition (mass%) Al₂O₃ 75.6, SiO₂ 24.3, $Na_2O 0.07$, CaO 0.02, MgO 0.05, $Fe_2O_3 0.03$, TiO₂ 0.04, ZrO₂ 0.03, true density 3.265 g/cm³, Kureha Chemical Industry Co. Ltd., Japan, powder 2 (Sol-gel process mullite)-median particle size 1.54 µm, chemical composition (mass%) Al₂O₃ 71.46, SiO₂ 28.13, ZrO₂ 0.30, TiO_2 0.10, Na₂O 0.01, specific surface area 7.7 m²/g, true density 3.169 g/cm³, isoelectric point pH 4.9, Chichibu Cement Ltd., Japan. In the fabrication of fully dense mullite (sample No. 1 in Tables 3 and 4), mullite powder 2 was dispersed in an aqueous solution at pH 3.0 adjusted with 1 M-HCl solution to prepare the suspension of 30 vol% solid. The acidic suspension of positively charged mullite particles was filtrated over a gypsum board into a cylindrical shape (diameter 10 mm) for the thermal conductivity measurement. The wet compacts were dried for 7 days at room temperature. The dried powder compacts were hot-pressed in a graphite mold at 1873 K for 2 h under a pressure of 39 MPa in an Ar atmosphere (FVPHP-5-R, Fuji Dempa Kogyo Co., Ltd., Osaka, Japan). The heating and cooling rates were both 10 K/min. In the fabrication of porous mullite compacts with various porosities (samples Nos. 2-7 in Tables 3, 4), the single mode mullite powder 2 (samples Nos. 3, 4, 5) and the bimodal mullite powder at the volume fraction of powder 1: powder 2=33: 67% (samples Nos. 2, 6, 7) were hot-pressed at 1673-1873 K under a lower pressure of 0.125 MPa in an Ar atmosphere for 1 h. In the processing of porous mullite with a further high porosity (samples Nos. 8-10 in Tables 3 and 4), the aqueous mullite suspension of power 2 was prepared at pH 7.0 at the solid content of 30 vol%, and consolidated to sinter at 1773 K in air for 1 h. The hot-pressed or pressureless-sintered mullite compacts were polished with SiC abrasive papers (80 µm SiC grains) into a disk shape with a diameter of 10 mm and a thickness of 2 mm. The fully dense mullite sample (No. 1) was annealed at 1273 K in air for 6 h to eliminate the residual thermal stress due to the hot-pressing. In the above preparation of porous mullite ceramics, 4-10 samples were sintered at the same time to examine their phase compositions, sintered densities, microstructures, pore size distributions and thermal conductivities. The difference in the relative densities of several mullite samples were less than ±3% against the average value. The slight difference in the notation of relative densities of mullite samples in the present figures is due to the above reason. The phases of the fabricated mullite samples were identified by X-ray diffraction analysis (RINT 2200, Rigaku Co. Ltd., Japan). The sintered density and porosity were measured by the Archimedes method using double-distilled water. The microstructures of sintered mullite were observed by scanning electron microscopy (SEM, JXA-8230, JEOL Ltd., Japan). The pore size distributions of porous mullite samples were measured by mercury porosimetry at Saga Ceramics Research Laboratory in Japan (Aritacho, Nishimatsuura-gun, Saga 844-0024, Japan). The heat capacity

and thermal diffusibility of the mullite samples (diameter 10 mm, thickness 2 mm) were measured at 298–1273 K by a laser flash method at Okayama Ceramics Research Foundation (1406-18 Nishikatakami, Bizen-shi, Okayama, Japan). A pulsed laser was irradiated on a sample surface. Then, the time-dependence of temperature at the opposite surface of sample was measured. Based on the time-dependence of temperature, the thermal diffusivity (α , m²/s) and specific heat capacity (C_{P2} , J/gK) were determined. The thermal diffusivity is expressed by Eq. (2),

$$\alpha = \frac{1.37L^2}{\pi^2 t_{1/2}}$$
(2)

where L and $t_{1/2}$ are the thickness of sample and the half of time until the surface temperature of sample reaches the maximum temperature. The C_{P2} value is expressed by Eq. (3) at room temperature and Eq. (4) at higher temperatures, respectively,

$$C_{P2, R} = \frac{1}{m} \left(\frac{Q}{\Delta T_{0, R}} - C_a m_a - C_b m_b \right)$$
(3)

$$C_{P2, T} = \frac{\Delta I_{0, R}}{\Delta T_{0, T}} C_{P2, R}$$
(4)

where m, m_a and m_b are the masses of sample, a laser absorber and an adhesive agent, respectively, C_a and C_b are the specific heat capacities of the laser absorber and the adhesive agent, respectively, Q the absorbed heat quantity, $\Delta T_{0, R}$ and $\Delta T_{0, T}$ are the parameters of the temperature relaxation curves at room temperature and higher temperatures, respectively. The thermal conductivity (κ , W/mK) is obtained by multiplying the thermal diffusivity (α , m²/s), specific heat capacity (C_{P2}, J/gK) and bulk density (ρ , g/m³).

$$\kappa = \alpha C_{P2} \rho = \alpha C_{P1} \ (C_{P1} = C_{P2} \rho, \ J/m^3 K)$$
(5)

3. Results and discussion

3.1. Influence of heating temperature on the thermal properties of porous mullite

The X-ray diffraction patterns of all the mullite samples in Table 3 indicated the formation of mullite single phase with no secondary phase. Fig. 1 shows the microstructures of mullite compacts with different porosities of (a) 0%, (b) 13.9%, (c) 37.1% and (d) 50.6% (sintered with samples Nos. 1, 2, 6 and 8 at the same time, respectively, in Table 3). The closed porosities of samples in Fig. 1(b), (c) and (d) were 1.1%, 1.1% and 6.5%, respectively. As the densification proceeded, the mullite particles were connected each other (Fig. 1(c) and (d)) and then dense solid parts without pores were formed spottedly (Fig. 1(b)). In Fig. 1(a), no significant pores were observed. Fig. 2 shows the pore size distributions of the porous mullite samples hotpressed at (a) 1673 K, (b) 1773 K and (c) 1873 K under a pressure of 0.125 MPa using the single mode and bimodal size mullite powders. As seen in Fig. 2, uniform pores with a narrow pore size distribution were contained in each mullite compact. Addition of powder 1 to powder 2 gave little influence on the median pore size except for the hot-pressing at 1873 K. Increase in the hot-pressing temperature from 1673 to 1773 K provided no significant influence on the pore size distributions of porous mullite compacts. However, the sinterability of the mullite powders was greatly enhanced at 1873 K. The porosity calculated from the cumulative pore volume and the true density (3.169 g/cm^3) of powder 2 was almost in agreement with the porosity measured by the Archimedes method using distilled water.

Fig. 3 shows the thermal diffusibility (α), heat capacity (C_{P1}) at a constant pressure (101.33 kPa) and thermal conductivity (κ = $C_{P1}\alpha$) measured for a porous mullite ceramics (52% porosity) and dense mullite (0% porosity). These measured values are listed in Table 1. The

Download English Version:

https://daneshyari.com/en/article/5437657

Download Persian Version:

https://daneshyari.com/article/5437657

Daneshyari.com